Chapter 2
Colloidal Semiconductor Nanocrystals

Abstract In this chapter, we review colloidal semiconductor nanocrystals (NCs) and their remarkable size-dependent properties. We emphasize on colloidal nanoplatelets and explain how they differ from NCs of other classes.

Keywords Semiconductor · Colloidal nanocrystals · Quantum dots · Quasi-2D nanoplatelets

The presence of man-made nanocrystals (NCs) can be traced back to as early as three millennia ago [1]. However, compared to this time scale, the achievement of their reproducible synthesis using colloidal chemistry three decades ago is quite recent [2]. This rather recent development, though, enabled an enormous leap in semiconductor optoelectronics ever since. After nearly 30 years of their first well-controlled synthetic introduction, intensive research keeps being conducted on studying, improving, and exploiting their efficiency and other properties, as well as their incorporation in optoelectrical applications.

The magnificence of NCs lies in their size-dependent physical properties. This size dependence can be best understood by the quantum confinement effect, which can be quantified to first order by treating the NC as a quantum well with a finite barrier potential. Even by ignoring the crystalline structure and the resulting periodic potential within the NC volume, this treatment is able to approximate the evolution of electronic states with the dimensions of the quantum well [3]. In general, quantum confinement starts to become observable when the dimensions of the NC are comparable to the exciton Bohr radius. As the size of the NC keeps shrinking, this will result in further separation of the energy levels of the system. In the case of semiconductors, the separation between the highest occupied energy band and the lowest unoccupied energy band, i.e. the bandgap, will increase with shrinking size. This has been schematically demonstrated in Fig. 2.1. Not only does the bandgap increase with reduced size but also the energy bands are discretized with increased separation between states as the NC shrinks. In addition to the modifications in the energy levels, uncertainty will be introduced in the momenta of electrons and holes due to

O. Erdem and H. V. Demir, *Oriented Self-Assembly of Colloidal Semiconductor Nanoplatelets on Liquid Interfaces*, Nanoscience and Nanotechnology,
https://doi.org/10.1007/978-981-19-7052-8_2

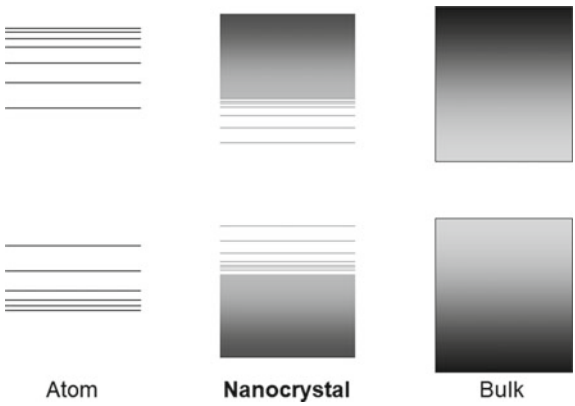

Fig. 2.1 Energy states of an atom, bulk crystal, and nanocrystal. Nanocrystals have discrete energy states near the highest occupied and lowest unoccupied molecular orbitals

their being localized within the NC volume, resulting in relaxation of the momentum conservation [4].

The work that pioneered the modern colloidal synthesis of semiconductor NCs came in 1993 by Murray et al. [2]. Herein, the formation of CdSe, CdS, or CdTe nanoparticles in colloidal medium is initiated by injection of Cd and Se (or S, Te) precursors into solution at an elevated temperature; these nuclei are grown until the desired size is reached and the growth is terminated by injecting organic ligands and lowering the reaction temperature. The resulting ensembles of CdSe spherical quantum dots (QDs) in this work have size dispersity as low as 5%, with the average QD size being tunable from 1.2 to 11.5 nm. The absorption onset of these CdSe QD ensembles is ~400 nm for the smallest average size and ~700 nm for the largest one [2].

An exemplary transmission electron micrograph of QDs is displayed in Fig. 2.2a. The crystallographic planes of the individual QDs are visible in the electron microscopy image. The crystalline structure is also depicted schematically in Fig. 2.2b. Typically, surface planes of these NCs are saturated by long-chain organic ligands. These organic ligands are used as a means to render the NC ensembles soluble in nonpolar organic solvents such as hexane and toluene. Additionally, they help with the passivation of the highly energetic, unsaturated bonds of the atoms on the NC surface. This kind of unsaturated bonds can be detrimental to the optical efficiency of NCs by resulting in charge trapping at the surface, which reduces the photoluminescence (PL) efficiency and the charge mobility, and therefore is undesirable in optical and photovoltaic applications [5]. Since the surface-to-volume ratio of the NCs is greatly enhanced in these nanometer-sized particles in comparison with bulk materials, loss of charge carriers and emission through surface trapping can significantly deteriorate the efficiency of these QDs, and saturation of the atomic bonds on the surface is essential.

The most common ligands are organic molecules with long hydrocarbon chains attached to a functional group. Examples of such ligands used in the NC synthesis include oleic acid [6, 7], trioctylphosphine [8, 9], and trioctylphosphine oxide [10].

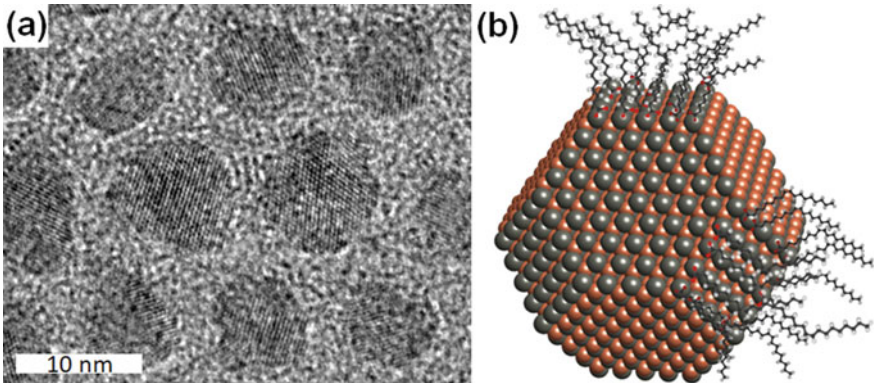

Fig. 2.2 **a** Transmission electron micrograph of CdZnS/ZnS quantum dots (2018 Demir Group). **b** Schematic depiction of a quasi-spherical colloidal CdSe nanocrystal capped with ligands (in this schematic, oleate) on facets. Ligands on some facets are not drawn for clarity purposes

In most cases, the functional group of these molecules is ionized in solution and attaches itself to the oppositely charged atoms on the surface [11].

It is also possible to bind inorganic ligands to the surface of QDs to achieve solubility in polar solvents. Approaches for QD synthesis in water-based environment [12] or post-synthesis procedures for replacing organic ligands with inorganic ones enable the making of water-soluble NCs [13, 14].

Today, synthesis of highly monodisperse QD ensembles with high PL efficiency and narrow emission linewidth is possible with the emission wavelength tunable through the entire visible spectrum and beyond. To this end, a variety of compositions, as well as heterostructures have been introduced. While Cd-based II–VI QDs are still being studied and used to a great extent, other compositions have been eventually introduced not long after CdX QDs. These compositions include III–V semiconductors such as InAs [9] and InP [15, 16] and IV–VI semiconductors such as PbS [6] and PbSe [17]. Owing to their much smaller bandgap than CdSe, the QDs of these other semiconductors are more suitable for the IR regime. Altogether, the spectral range of QDs made of these material systems can extend from visible to IR (up to 3.5 μm) [18, 19].

Even more common than the single-composition QDs (Fig. 2.3a) are the QD heterostructures, where the "core" QD is enclosed by a "shell" to increase the surface passivation and prevention of leakage of the excitonic wavefunction outside the QD volume (Fig. 2.3b). With such heterostructures as CdSe/CdS [20, 21], CdSe/ZnS [22, 23] and InP/ZnS [24, 25] more stable solutions and better quantum yield is achieved compared with core-only QDs. It is also possible to create a potential gradient between the core and shell, where the molecular composition changes gradually from the center to the outermost shell (Fig. 2.3c) [26–28].

Colloidal QDs have advantageous properties including but not limited to emission/absorption tunability, solution processability, and large absorption cross-section. Furthermore, as their sizes are orders of magnitude smaller than light wavelength,

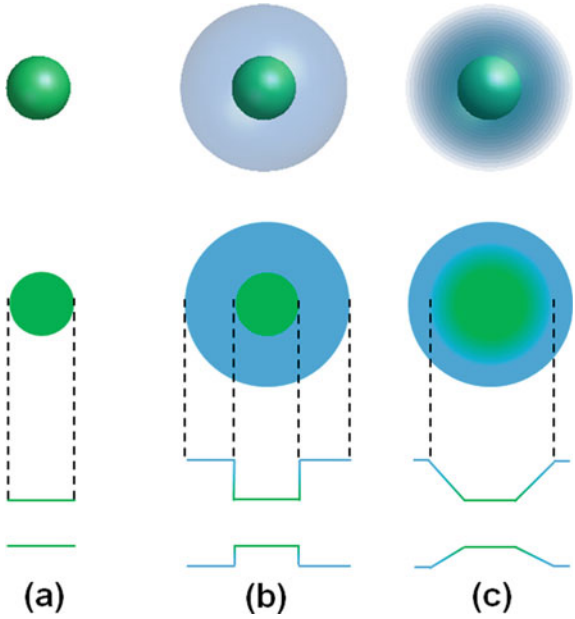

Fig. 2.3 Two-and three-dimensional schematics for **a** core, **b** core/shell, and **c** gradient core/shell QDs. Depending on the selected pair of compositions, the valence and conduction band offsets of core and (gradient) shell may vary

they do not induce scattering individually while interacting with light. These properties render them especially favorable in optoelectrical devices. Applications including light-emitting diodes (LEDs) [29], lasers [10, 30], and field effect transistors [31] have already benefited from the favorable features of these tunable nanoemitters.

Readers interested in a detailed overview of the synthesis and applications of various NCs are referred to [19, 32]. A theoretical treatment of semiconductor NCs can be found in [3, 33].

2.1 Colloidal Quantum Wells (Nanoplatelets)

Apart from the deeply investigated spherical QDs, colloidal NCs of various shapes and dimensionalities have also been eventually reported and studied. These include nanocubes [34], tetrapods [35, 36] and quasi-one-dimensional (1D) nanorods [37, 38]. In the last decade, a new class of colloidal NCs has been introduced, which is the quasi-two-dimensional nanoplatelets (NPLs) with one-dimensional quantum confinement [39, 40].

Colloidal NPLs have lateral sizes ranging from several nm to about 100 nm while having a thickness of only a few atoms. This means that, unlike spherical, quasi-0D QDs, where the quantum confinement is 3D, NPLs have effective quantum confinement only along the vertical direction. The thickness of the NPL therefore determines the strength of quantum confinement, and, in turn, the bandgap.

The most remarkable property of the NPLs is that their lateral surfaces are atomically flat with no variation in thickness. Owing to this atomic precision in their thickness, their ensembles have little or no inhomogeneous broadening. NPLs can thus have emission linewidths as small as several nms [39] at room temperature, which has not been possible with QDs even in their highly monodisperse ensembles.

The presence of NPLs has been observed in the early 2000s as ultra-narrow features in absorption and emission features of colloidal NC ensembles. Initially, these features have been attributed to "magic-sized" nanoclusters in the ensemble with discrete sizing [41, 42]. At the end of the decade, Ithurria et al. managed to reproducibly synthesize these discretely sized CdX (X = Se, S, Te) NCs, not as a by-product, but as the main output of their synthesis procedure. Their seminal work demonstrated that NPLs are atomically flat with one-dimensional quantum confinement, giant oscillator strength, and ultranarrow emission linewidth [39, 40].

In Fig. 2.4a, individual CdSe NPLs of different thicknesses are drawn schematically. The crystal structure of a NPL is composed of alternating atomic planes of Cd and Se, the bottom- and topmost layers always being a Cd plane. Thus, for N layers of Se planes in an NPL, there will be $N + 1$ Cd planes. In this case, the thickness of the NPL can be expressed as N monolayers (ML), where a "monolayer" represents a Cd-Se atomic pair along the vertical direction. It is also not uncommon to use half-integers as the number of monolayers, to signify the presence of the extra Cd atomic plane. Throughout this brief, we use this latter nomenclature when referring to the core NPL thicknesses.

Figure 2.4b displays the scanning transmission electron micrograph of 5.5 ML CdSe NPLs. For most of the NPLs in the image, the visible surface is a lateral one. In Fig. 2.4c, absorption and photoluminescence spectra of 3.5, 4.5, and 5.5 ML NPL ensembles are plotted. The sharp excitonic features can be discerned in these spectra, which correspond to the electron-heavy hole and electron-light hole transitions. The Stokes shift between the emission and absorption peaks is exceptionally low, typically limited to a few nm [39]. It is also seen here that the atomically flat thickness and the confinement energy being essentially determined by only one dimension comes at the cost of the discretization of spectral tunability. In contrast to QDs, where the excitonic features can be continuously tuned by size engineering, the size-dependent absorption peak leaps from ~460 to 510 nm when the NPL thickness is increased from 3.5 to 4.5 ML, and to 553 nm when it is further increased by another ML. This limitation in tunability can be largely overcome by various approaches such as compositional alloying [43, 44], making heterostructures and to a limited extent, enforcing additional quantum confinement along one of the two lateral dimensions, i.e. making the size along that lateral dimension comparable to the exciton Bohr radius [45, 46].

To date, the synthesis of NPLs with thicknesses ranging from 2.5 to 9.5 ML has been reported [39, 46–51]. In addition, similar to QDs, making heterostructures of NPLs is also possible for purposes of improved colloidal stability and photoluminescence efficiency. However, unlike QDs, where the only possibility is growing a radial shell, there are two degrees of freedom when shelling NPLs, namely the growth of lateral wings around the periphery of the NPL, and sandwiching the core NPL by

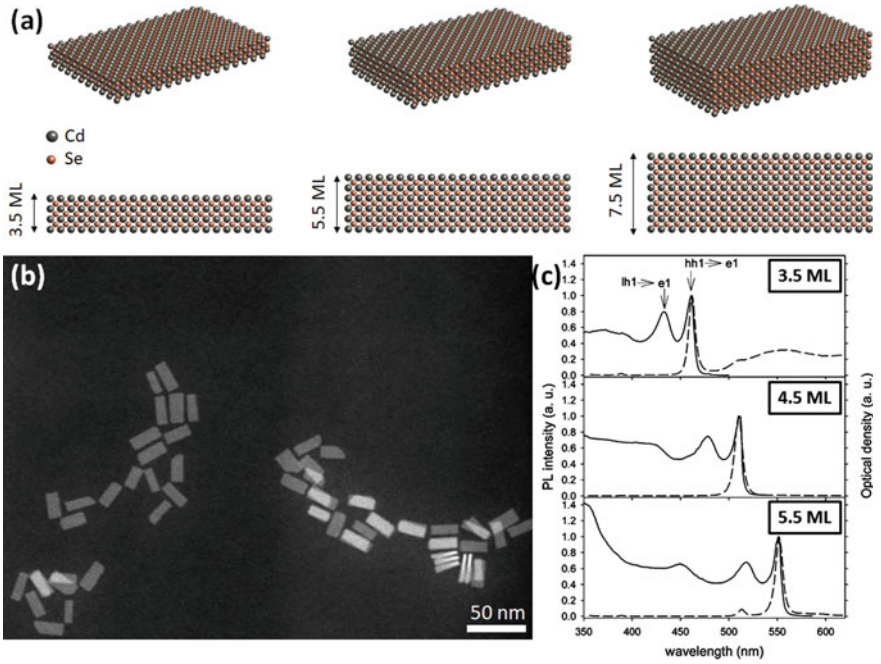

Fig. 2.4 **a** Schematic drawing of 3.5, 5.5 and 7.5 ML CdSe zinc-blend nanoplatelets (NPLs). **b** Scanning transmission electron micrograph of 5.5 ML NPLs (2017 Demir Group). **c** Absorbance (solid line) and PL (dashed line) spectra of 3.5, 4.5, and 5.5 ML CdSe NPLs. Adapted with permission from [40]. Copyright 2008 American Chemical Society

shelling it vertically and surrounding a little bit around the periphery as well. These heterostructures, commonly known as core/crown [52, 53] and core/shell NPLs, respectively, are schematically depicted in Fig. 2.5. It is also possible to combine these two shelling methods to obtain core/crown/shell NPLs [54].

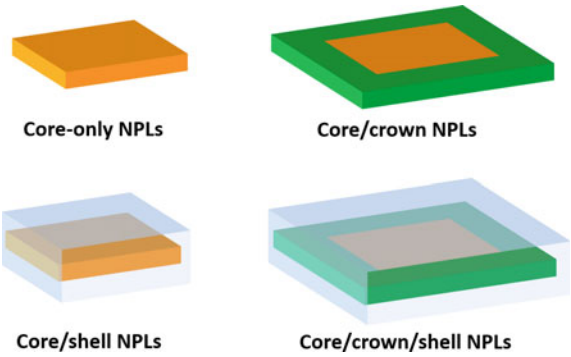

Fig. 2.5 Schematics of core, core/shell, core/crown, and core/crown/shell NPLs

NPLs have already been demonstrated to be suitable for optoelectronics applications such as LEDs [43, 55], solar concentration [56], and lasing [57–59], in most cases outperforming their quantum-dot counterparts. This superior performance is thanks to their enhanced absorption, giant oscillator strength, and lack of inhomogeneous broadening.

Another striking property of the NPLs is the anisotropy of the band-edge excitonic dipole, which leads to directional emission out of NPLs [60]. Such directionality is essential for the active media of LEDs and lasers and is one of the main motivations for controlling the orientation of NPLs collectively in their ensemble. Methods of orientation control of NPLs and their use in optoelectronic applications will be discussed in detail in Chap. 4 and 5.

For a more detailed overview of colloidal NPLs, a number of reviews are available that cover early and more recent progress on synthesis, optical properties, and potential applications [32, 53, 61, 62].

References

1. Montanarella F, Kovalenko MV (2022) Three millennia of nanocrystals. ACS Nano 16:5085–5102
2. Murray CB, Norris DJ, Bawendi MG (1993) Synthesis and characterization of nearly monodisperse CdE (E = sulfur, selenium, tellurium) semiconductor nanocrystallites. J Am Chem Soc 115:8706–8715
3. Gaponenko SV (1998) Optical properties of semiconductor nanocrystals. Cambridge University Press, Cambridge
4. Alivisatos AP (1996) Perspectives on the physical chemistry of semiconductor nanocrystals. J Phys Chem 100:13226–13239
5. Kambhampati P (2011) Hot exciton relaxation dynamics in semiconductor quantum dots: radiationless transitions on the nanoscale. J Phys Chem C 115:22089–22109
6. Hines MA, Scholes GD (2003) Colloidal PbS nanocrystals with size-tunable near-infrared emission: observation of post-synthesis self-narrowing of the particle size distribution. Adv Mater 15:1844–1849
7. Schliehe C, Juarez BH, Pelletier M et al (2011) Ultra-thin PbS sheets by two-dimensional oriented attachment. Science 74:550–554
8. Dabbousi BO, Murray CB, Rubner MF, Bawendi MG (1994) Langmuir-Blodgett manipulation of size-selected cdse nanocrystallites. Chem Mater 6:216–219
9. Guzelian AA, Banin U, Kadavanich AV et al (1996) Colloidal chemical synthesis and characterization of InAs nanocrystal quantum dots. Appl Phys Lett 69:1432–1434
10. Klimov VI, Mikhailovsky AA, Xu S et al (2000) Optical gain and stimulated emission in nanocrystal quantum dots. Science 290:314–317
11. Hens Z, Martins JC (2013) A solution NMR toolbox for characterizing the surface chemistry of colloidal nanocrystals. Chem Mater 25:1211–1221
12. Gaponik N, Talapin DV, Rogach AL et al (2002) Thiol-capping of CDTe nanocrystals: an alternative to organometallic synthetic routes. J Phys Chem B 106:7177–7185
13. Dubois F, Mahler B, Dubertret B et al (2007) A versatile strategy for quantum dot ligand exchange. J Am Chem Soc 129:482–483
14. Kovalenko MV, Scheele M, Talapin DV (2009) Colloidal nanocrystals with molecular metal chalcogenide surface ligands. Science 324:1417–1420
15. Mićić OI, Curtis CJ, Jones KM et al (1994) Synthesis and characterization of InP quantum dots. J Phys Chem 98:4966–4969

16. Mićić OI, Curtis CJ, Jones KM et al (1995) Synthesis and characterization of InP, GaP and GaInP2 quantum dots. J Phys Chem 99:7754–7759
17. Murray CB, Sun S, Gaschler W et al (2001) Colloidal synthesis of nanocrystals and nanocrystal superlattices. IBM J Res Dev 45:47–56
18. Rogach AL, Eychmüller A, Hickey SG, Kershaw SV (2007) Infrared-emitting colloidal nanocrystals: synthesis, assembly, spectroscopy, and applications. Small 3:536–557
19. Talapin DV, Lee J-S, Kovalenko MV, Shevchenko EV (2009) Prospects of colloidal nanocrystals for electronic and optoelectronic applications. Chem Rev 110:389–458
20. Peng X, Schlamp MC, Kadavanich AV, Alivisatos AP (1997) Epitaxial growth of highly luminescent CdSe/CdS core/shell nanocrystals with photostability and electronic accessibility. J Am Chem Soc 119:7019–7029
21. Revaprasadu N, Malik MA, O'Brien P, Wakefield G (1999) A simple route to synthesise nanodimensional CdSe-CdS core-shell structures from single molecule precursors. Chem Commun 1573–1574
22. Talapin DV, Rogach AL, Kornowski A et al (2001) Highly luminescent monodisperse CdSe and CdSe/ZnS nanocrystals synthesized in a hexadecylamine-trioctylphosphine oxide-trioctylphospine mixture. Nano Lett 1:207–211
23. Shevchenko EV, Weller H, Rogach BAL et al (2002) Organization of matter on different size scales: monodisperse nanocrystals and their superstructures. Adv Funct Mater 12:653–664
24. Li L, Reiss P (2008) One-pot synthesis of highly luminescent InP/ZnS nanocrystals without. J Am Chem Soc 130:11588–11589
25. Ramasamy P, Kim B, Lee MS, Lee JS (2016) Beneficial effects of water in the colloidal synthesis of InP/ZnS core-shell quantum dots for optoelectronic applications. Nanoscale 8:17159–17168
26. Boldt K, Kirkwood N, Beane GA, Mulvaney P (2013) Synthesis of highly luminescent and photo-stable, graded shell CdSe/Cd xZn1-xS nanoparticles by in situ alloying. Chem Mater 25:4731–4738
27. Lee KH, Lee JH, Song WS et al (2013) Highly efficient, color-pure, color-stable blue quantum dot light-emitting devices. ACS Nano 7:7295–7302
28. Wu K, Park Y-SS, Lim J, Klimov VI (2017) Towards zero-threshold optical gain using charged semiconductor quantum dots. Nat Nanotechnol 12:1140–1147
29. Shirasaki Y, Supran GJ, Bawendi MG, Bulovic V (2013) Emergence of colloidal quantum-dot light-emitting technologies. Nat Photonics 7:13–23
30. Dang C, Lee J, Breen C et al (2012) Red, green and blue lasing enabled by single-exciton gain in colloidal quantum dot films. Nat Nanotechnol 7:335–339
31. Hetsch F, Zhao N, Kershaw SV, Rogach AL (2013) Quantum dot field effect transistors. Mater Today 16:312–325
32. Kovalenko MV, Manna L, Cabot A et al (2015) Prospects of nanoscience with nanocrystals. ACS Nano 9:1012–1057
33. Klimov VI (2017) Nanocrystal quantum dots, 2nd edn. CRC Press, Boca Raton, FL
34. Yu R, Ren T, Sun K et al (2009) Shape-controlled copper selenide nanocubes synthesized by an electrochemical crystallization method. J Phys Chem C 113:10833–10837
35. Manna L, Milliron DJ, Meisel A et al (2003) Controlled growth of tetrapod-branched inorganic nanocrystals. Nat Mater 2:382–385
36. Milliron DJ, Hughes SM, Cui Y et al (2004) Colloidal nanocrystal heterostructures with linear and branched topology. Nature 430:190–195
37. Peng X, Manna L, Yang W et al (2000) Shape control of CdSe nanocrystals. Nature 404:59–61
38. Talapin DV, Nelson JH, Shevchenko EV et al (2007) Seeded growth of highly luminescent CdSe/CdS nanoheterostructures with rod and tetrapod morphologies. Nano Lett 7:2951–2959
39. Ithurria S, Tessier MD, Mahler B et al (2011) Colloidal nanoplatelets with two-dimensional electronic structure. Nat Mater 10:936–941
40. Ithurria S, Dubertret B (2008) Quasi 2D colloidal CdSe platelets with thicknesses controlled at the atomic level. J Am Chem Soc 130:16504–16505
41. Peng ZA, Peng X (2002) Nearly monodisperse and shape-controlled CdSe nanocrystals via alternative routes: nucleation and growth. J Am Chem Soc 124:3343–3353

42. Ouyang J, Zaman MB, Yan FJ et al (2008) Multiple families of magic-sized CdSe nanocrystals with strong bandgap photoluminescence via noninjection one-pot syntheses. J Phys Chem C 112:13805–13811
43. Fan F, Kanjanaboos P, Saravanapavanantham M et al (2015) Colloidal $CdSe_{1-x}S_x$ nanoplatelets with narrow and continuously-tunable electroluminescence. Nano Lett 15:4611–4615
44. Kelestemur Y, Dede D, Gungor K et al (2017) Alloyed heterostructures of CdSe x S 1–x nanoplatelets with highly tunable optical gain performance. Chem Mater 29:4857–4865
45. Bertrand GHV, Polovitsyn A, Christodoulou S et al (2016) Shape control of zincblende CdSe nanoplatelets. Chem Commun 52:11975–11978
46. Di Giacomo A, Rodà C, Khan AH, Moreels I (2020) Colloidal synthesis of laterally confined blue-emitting 3.5 monolayer CdSe nanoplatelets. Chem Mater 32:9260–9267
47. Delikanli S, Yu G, Yeltik A et al (2019) Ultrathin highly luminescent two-monolayer colloidal CdSe nanoplatelets. Adv Funct Mater 29:1901028
48. İzmir M, Sharma A, Shendre S et al (2022) Blue-emitting CdSe nanoplatelets enabled by sulfur-alloyed heterostructures for light-emitting diodes with low turn-on voltage. ACS Appl Nano Mater 5:1367–1376
49. Cho W, Kim S, Coropceanu I et al (2018) Direct synthesis of six-monolayer (1.9 nm) thick zinc-blende CdSe nanoplatelets emitting at 585 nm. Chem Mater 30:6957–6960
50. Ji B, Rabani E, Efros AL et al (2020) Dielectric confinement and excitonic effects in two-dimensional nanoplatelets. ACS Nano 14:8257–8265
51. Moghaddam N, Dabard C, Dufour M et al (2021) Surface modification of CdE (E: S, Se, and Te) nanoplatelets to reach thicker nanoplatelets and homostructures with confinement-induced intraparticle type I energy level alignment. J Am Chem Soc 143:1863–1872
52. Prudnikau A, Chuvilin A, Artemyev M (2013) CdSe−CdS nanoheteroplatelets with efficient photoexcitation of central CdSe region through epitaxially grown CdS wings. J Am Chem Soc 135:14476–14479
53. Lhuillier E, Pedetti S, Ithurria S et al (2015) Two-dimensional colloidal metal chalcogenides semiconductors: synthesis, spectroscopy, and applications. Acc Chem Res 48
54. Kelestemur Y, Guzelturk B, Erdem O et al (2016) Platelet-in-box colloidal quantum wells: CdSe/CdS@CdS Core/Crown@Shell heteronanoplatelets. Adv Funct Mater 26:3570–3579
55. Liu B, Altintas Y, Wang L, et al (2020) Record high external quantum efficiency of 19.2% achieved in light-emitting diodes of colloidal quantum wells enabled by hot-injection shell growth. Adv Mater 32:1905824
56. Sharma M, Gungor K, Yeltik A et al (2017) Near-unity emitting copper-doped colloidal semiconductor quantum wells for luminescent solar concentrators. Adv Mater 29:1–10
57. She C, Fedin I, Dolzhnikov DS et al (2014) Low-threshold stimulated emission using colloidal quantum wells. Nano Lett 14:2772–2777
58. Guzelturk B, Kelestemur Y, Olutas M et al (2014) Amplified spontaneous emission and lasing in colloidal nanoplatelets. ACS Nano 8:6599–6605
59. She C, Fedin I, Dolzhnikov DS et al (2015) Red, yellow, green, and blue amplified spontaneous emission and lasing using colloidal CdSe nanoplatelets. ACS Nano 9:9475–9485
60. Gao Y, Weidman MC, Tisdale WA (2017) CdSe nanoplatelet films with controlled orientation of their transition dipole moment. Nano Lett 17:3837–3843
61. Yu J, Chen R (2020) Optical properties and applications of two-dimensional CdSe nanoplatelets. InfoMat 2:905–927
62. Sharma M, Delikanli S, Demir HV (2020) Two-dimensional CdSe-based nanoplatelets: their heterostructures, doping, photophysical properties, and applications. Proc IEEE 108:655–675